Biosensors and Bioelectronics 64 (2015) 566–571

Contents lists available at ScienceDirect

Biosensors and Bioelectronics

journal homepage: www.elsevier.com/locate/bios

Ultrasensitive electrochemical detection of avian influenza A (H7N9) virus DNA based on isothermal exponential amplification coupled with hybridization chain reaction of DNAzyme nanowires

Yanyan Yu [a], Zuanguang Chen [a,*], Wensi Jian [a], Duanping Sun [a], Beibei Zhang [a], Xinchun Li [b], Meicun Yao [a,*]

[a] School of Pharmaceutical Sciences, Sun Yat-sen University, Guangzhou 510006, China
[b] School of Pharmaceutical Sciences, Guangxi Medical University, Nanning 530021, China

ARTICLE INFO

Article history:
Received 2 August 2014
Received in revised form
18 September 2014
Accepted 29 September 2014
Available online 2 October 2014

Keywords:
Electrochemical biosensor
Exponential amplification reaction
Hybridization chain reaction
H7N9
G-quadruplex

ABSTRACT

In this work, a simple and label-free electrochemical biosensor with duel amplification strategy was developed for DNA detection based on isothermal exponential amplification (EXPAR) coupled with hybridization chain reaction (HCR) of DNAzymes nanowires. Through rational design, neither the primer nor the DNAzymes containing molecular beacons (MBs) could react with the duplex probe which were fixed on the electrode surface. Once challenged with target, the duplex probe cleaved and triggered the EXPAR mediated target recycle and regeneration circles as well as the HCR process. As a result, a greater amount of targets were generated to cleave the duplex probes. Subsequently, the nanowires consisting of the G-quadruplex units were self-assembled through hybridization with the strand fixed on the electrode surface. In the presence of hemin, the resulting catalytic G-quadruplex–hemin HRP-mimicking DNAzymes were formed. Electrochemical signals can be obtained by measuring the increase in reduction current of oxidized 3.3′,5.5′-tetramethylbenzidine sulfate (TMB), which was generated by DNAzyme in the presence of H_2O_2. This method exhibited ultrahigh sensitivity towards avian influenza A (H7N9) virus DNA sequence with detection limits of 9.4 fM and a detection range of 4 orders of magnitude. The biosensor was also capable of discriminating single-nucleotide difference among concomitant DNA sequences and performed well in spiked cell lysates.

1. Introduction

Sensitive detection of specific DNA sequences has attracted substantial research efforts due to the broad possible applications in genetic research of diseases, clinical diagnosis, and clinical therapy (Lubin and Plaxco, 2010; Sassolas et al., 2008). A number of techniques such as molecular biology (Dervan, 2001; Keren et al., 2002; Shen et al., 2014), electrochemistry (Lu et al., 2012; Xia et al., 2010), spectroscopy (Pan et al., 2013; Wang et al., 2014a) and colorimetry (Zhang et al., 2012) have been applied to achieve sensitive detection of nucleic acids. Up to now, various signal amplification strategies have been developed for the ultrasensitive sequence-specific detection of DNA. Typically, the cycling methods via nuclease, e.g., exonuclease (Xuan et al., 2013; Zhou et al., 2014a), polymerase (Hun et al., 2013; Shi et al., 2014) and endonuclease (Duan et al., 2013; Wang and Zhang, 2012) have been widely employed to realize the trace level detection of target DNA. Notably, the isothermal exponential amplification reaction (EXPAR), by combination of polymerase strand extension and single-strand nicking, has gained great attention in profiling low-abundance DNA because of its high sensitivity, low cost and good tolerance to the inhibitory components in the clinical samples. EXPAR has the intrinsic merits of isothermal nature, high amplification efficiency and rapid amplification kinetics, which can provide 10^6–10^9 fold amplification within minutes under isothermal conditions. In addition, metal nanoparticles (Sharifi et al., 2014; Wu et al., 2014), quantum dots (Zhu et al., 2014), DNA biobarcode (Xu et al., 2012; Zhou et al., 2014b) and labeled enzymes (Ge et al., 2014) were also the common examples of amplification strategy. However, the multiple assay steps, the addition of many exogenous reagents and the labeling process made them laborious and costly. Catalytic nucleic acids (DNAzymes or ribozymes) (Willner et al., 2008), on the other hand, has gained growing interest as amplifying labels. The flexible base sequences, isothermal reaction and reduced nonspecific binding properties provided unique features for bioanalytical applications.

* Corresponding authors. Fax: +86 20 39943071.
E-mail addresses: chenzg@mail.sysu.edu.cn (Z. Chen), yaomeicun@gmail.com (M. Yao).

http://dx.doi.org/10.1016/j.bios.2014.09.080
0956-5663/

Specifically, the G-quadruplex–hemin horseradish peroxidase (HRP)-mimicking enzyme has been extensively used as a catalytic label for the amplified colorimetric (Li et al., 2009; Zhu et al., 2011), electrochemical (Wang et al., 2013; Wang et al., 2014b) or chemiluminescent (Gao and Li, 2013; Luo et al., 2012; Zhou et al., 2012) detection of DNA. By combination with hybridization chain reaction (HCR) to assemble long nanowires or rolling circle amplification strategy, G-quadruplex–hemin complex itself can achieve the signal amplification process efficiently (Cheglakov et al., 2007; Shimron et al., 2012; Wang et al., 2014a; Weizmann et al., 2006).

In the present work, we developed an ultrasensitive and label-free electrochemical DNA biosensor with isothermal dual-amplification strategy based on EXPAR coupled with HCR of DNAzymes nanowires. The target recycle and self-assemble amplification processes can take place in succession at isothermal condition. Electrochemical methods, with high portability and affordability, were particularly attractive for nucleic acid detection. The integration of duel amplification strategy with the merits of electrochemical detection was supposed to achieve ultrasensitive electrochemical nucleic acid detection. Single stranded DNA derived from hemagglutinin (HA)-encoding sequences from avian influenza A (H7N9) virus was chosen as the target. Without the target, the molecular beacons (MBs) containing the G-quadruplex forming region cannot be opened up or assembled together. The duplex probe fixed on the surface of the electrode consisted of two sequences that were partially complementary with each other. The amplification strategy was initiated by the hybridization of the target DNA with one sequence of the probe. After cleavage of the probe through toehold mediated strand displacement (TMSDR), the target containing duplex was released to the solution and triggered the EXPAR. The other strand of the probe assembled on the electrode can then hybridize with MBs and open the hairpin structure through TMSDR, resulting in an autonomous stem-opening process that yields the formation of G-quadruplex nanowires. Due to the duel amplification process, the biosensor we fabricated can achieve ultrasensitive detection of DNA down to 9.4 fM and also performs well in single nucleotide polymorphism (SNP) discrimination and spiked cell lysates analysis.

2. Experimental

2.1. Chemicals and materials

DNA sequences were synthesized from Sangon Biotech. Co., Ltd. (Shanghai, China). The Bst DNA polymerase, Large Fragment, Nt. BspQI nicking endonuclease, deoxynucleotide solution mixture (dNTPs) and CutSmart Buffer were purchased from New England Biolabs (Beijing, China). Hemin, H_2O_2 (30%), tris(2-carboxyethy) phosphine hydrochloride (TCEP), 4-(2-hydroxyethyl) piperazine-1-ethanesulfonic acid sodium salt (HEPES) and dimethyl sulfoxide (DMSO) were obtained from Aladin Chemistry Co. Ltd. (Shanghai, China). 6-Mercapto-1-hexanol (MCH) was from J&K Scientific Ltd. (Guangzhou, China). One mM MCH solution was made by dilution of the MCH with DNA hybridization buffer (20 mM HEPES, 500 mM NaCl, pH 7.4). A stock solution of hemin (10 mM) was prepared in DMSO and stored in the dark at −20 °C. All DNA sequences were diluted in 1 × TE buffer (pH 8.0) to give stock solutions of 100 μM. Sequences of the oligonucleotides were designed with the help of online software (from the Web site of Integrated DNA Technologies (IDT)), as listed in Table S1.

2.2. Biosensor fabrication

The gold electrode (3 mm in diameter) was cleaned by immersion in a freshly prepared piranha solution (a 3:1 v/v mixture of concentrated H_2SO_4 and 30% H_2O_2) for 20 min, followed by a thorough rinse with ultrapure water. *CAUTION: Piranha solution reacts violently with organic materials; it must be handled with extreme care*. Then, the electrode was polished with 0.05 μm alumina slurry to obtain a mirror surface, followed by sonication in ethanol and ultrapure water for 5 min each to remove residual alumina powder. The electrode was then electrochemically cleaned over the potential between −0.2 and 1.5 V in H_2SO_4 (0.5 M) at a scan rate of 100 mV s^{-1} until a stable cyclic voltammogram was obtained. The gold electrode was rinsed with a copious amount of ultrapure water before it was blow-dried with nitrogen.

The duplex probes were prepared by mixing the same concentration of S1 and S2 in hybridization buffer. The solution was incubated at 90 °C for 5 min and then was allowed to cool to room temperature for at least 2 h. The MBs were also annealed through the same procedure. The duplex probe was incubated with 1 mM TCEP for 1 h to reduce disulfide bonds before assembled onto the electrode. The pretreated gold electrode was subjected to the above probe solution at 4 °C for 12 h and then was thoroughly rinsed with hybridization buffer. After drying with nitrogen, the electrode was immersed in 1 mM MCH solution subsequently for 1 h to remove the nonspecific DNA adsorption. Then, the electrode surface was rinsed and dried.

2.3. Electrochemical measurement and apparatus

Electrochemical experiments were conducted on RST5200F electrochemical workstation (Suzhou Risetest Instrument Co., Ltd., Suzhou, China). A three-electrode system consisting of a bare or modified gold electrode, an Ag/AgCl reference electrode and a platinum plate counter electrode, was employed in all electrochemical measurements. The differential pulse voltammetry (DPV) was performed with the potential window from 0.45 to 0.2 V in 20 mM HEPES buffer (pH 6.5, 50 mM KCl and 500 mM NaCl) containing 3.3′,5.5′-tetramethylbenzidine sulfate (TMB) (4 mM) and H_2O_2 (1 mm). The modified electrode was immersed into the HEPES buffer where the subsequent enzymatic reaction steps take place. The DPV was conducted after 1 min of catalytic reaction.

2.4. Dual-amplification process

Firstly, the probe modified gold electrode was incubated into 50 μL CutSmart Buffer containing 32 U Bst DNA polymerase, 20 U nicking endonuclease, 400 μM dNTPs, 2 μM primer, and different concentrations of target DNA for 90 min at 30 °C to conduct EXPAR. After being rinsed with HEPES buffer, the electrode was then incubated with the mixture of 2 μM MB1 and 2 μM MB2 for HCR to assemble the nanowires onto the cleaved probe. After 1 h, the resulting electrode was thoroughly rinsed before being subjected to 0.1 mM hemin in 20 mM HEPES buffer (pH 8.0, 50 mM KCl, 250 mM NaCl, 1% DMSO) for 30 min to induce the formation of G-quadruplex–hemin complexes.

3. Results and discussion

3.1. Principle of the biosensor for DNA detection

This newly designed electrochemical biosensor with dual-amplification strategy based on EXPAR coupled with HCR of

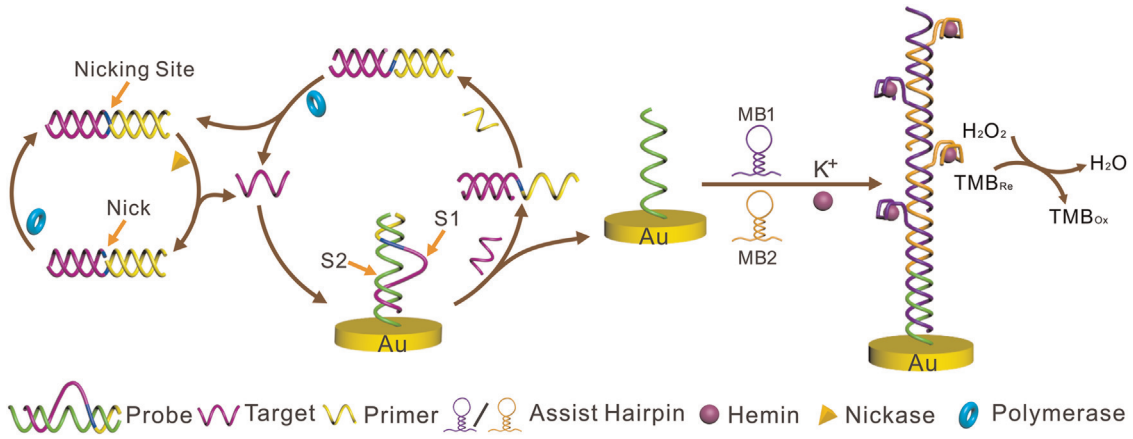

Scheme 1. Schematic illustration of dual amplification strategy based on EXPAR coupled with HCR of DNAzymes nanowires for electrochemical DNA assay. (For interpretation of the references to color in this figure legend, the reader is referred to the web version of this article.)

DNAzymes was illustrated in Scheme 1. The electrochemical biosensing process could be divided into two stages: EXPAR mediated target recycling and self-assemble of G-quadruplex. The probe consisted of two strands (S1 and S2, as shown in Table S1). The two sequences were designed as blockers to each other with a loop in the middle of S1. S2 prevented the hybridization of primer with S1. On the other hand, S1 stopped the hybridization of MBs to S2. The nicking site of nicking endonuclease was located in the loop region of S1 (blue region) and was an unsuitable substrate to the enzyme. Target DNA can hybridize to the 5′ stem region and part of loop region of S1 (purple region). The formation of target–substrate complex through TMSDR resulted in the thermal melting of the duplex (Li et al., 2007; Xiao et al., 2007). After cleavage of the probe, S2 was free to bind the MBs and triggered the HCR process. As the S1–target complex was released to the solution, after the hybridization of primer with the complementary region of S1 (yellow part), the polymerase initiated the polymerization, regenerating the target and synthesizing a DNA duplex. Once nicking endonuclease nicked at the DNA duplex, the polymerization proceeded and the primer part got extended again, regenerating a new target. Through the polymerase initiated polymerization and nicking endonuclease resulted nicks, target DNA was recycled and regenerated circularly. The released target DNA can hybridize with the probe and initiate another series of cyclic amplification recycle process. On the other hand, S2 was also released after each target binding and probe cleavage process, which can hybridize with the toehold of MB1 to open the hairpin structure. The yielding structure subsequently opened MB2 through strand displacement. By the autonomous opening of MB1 and MB2, polymer nanowires consisting of the G-quadruplex units were assembled on the electrode surface and in the presence of hemin the catalytic G-quadruplex–hemin HRP-mimicking DNAzymes were formed. Electrochemical signals can be got by measuring the increase in reduction current generated by oxidized TMB, which was generated by DNAzyme in the presence of H_2O_2.

3.2. Electrochemical characterization of the dual-amplification strategy

DPV was utilized to verify the feasibility of designed amplification process. As depicted in Fig. 1, a well-defined reduction peak around 0.3 V can be observed in the presence of 50 pM DNA after duel amplification process (curve e), which can be contributed to the reduction current generated by oxidized TMB generated from DNAzyme (Ahirwal and Mitra, 2010; Liu et al., 2008; Wan et al., 2013). In contrast, the DPV peak from the target without

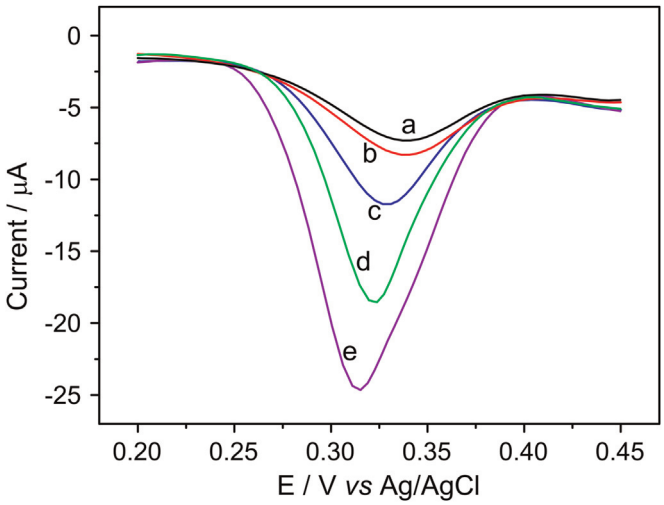

Fig. 1. Differential pulse voltammograms of blank control (a), 50 pM DNA without amplification (b), with HCR only (c) with EXPAR only (d) and with duel amplification (e).

amplification (curve b) was just a little higher than that from the blank control (curve a) whose response can be ascribed to the reduction of original oxidized TMB in the buffer. The greatly enhanced current in curve e affirmed that many more DNAzymes had been assembled on the electrode surface after duel amplification process. As the amplification strategy consisted of two processes, for the proof-of-concept experiment, we carried out experiments to investigate the effect of single reaction. If only HCR proceeded, without primer or enzymes, we can see from curve c that the electrochemical response raised obviously compared with curve b. While the EXPAR alone (curve d), which can be realized without addition of MB2 so that the DNAzyme nanowire cannot be extended, yielded even stronger response than HCR. This result may be attributed to the higher efficiency of the EXPAR. The peak current resulted from duel amplification was the highest among them demonstrating that the most DNAzymes were assembled on the electrode surface to catalyze the oxidation of TMB through this way.

3.3. Optimization of the dual-amplification strategy

Since DNA hybridization efficiency is a key factor for the electrode performance, we investigated the immobilization concentration of duplex DNA probe (0, 0.4, 0.8, 1.2, 1.6, and 2.0 μM) firstly. The result in Fig. 2A showed that the immobilization

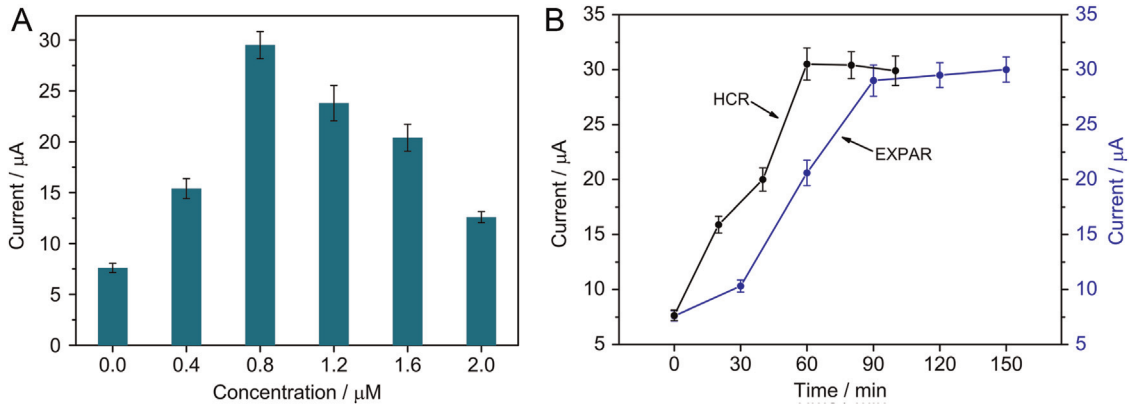

Fig. 2. (A) Effect of the probe concentration on the performance of the biosensor for detection of 100 pM DNA. (B) Effects of the reaction time of EXPAR and HCR on the performance of the biosensor for detection of 100 pM DNA. The data depicted the averages of three experiments and the error bars represented the standard deviation of three trials.

concentration of 0.8 μM gave the best performance. The higher immobilization concentration of probe can yield more denser DNA on the electrode surface, whereas it gave rise to greater steric hindrance effect as well, which may restrict the hybridization efficiency of target and the effective assembling of DNAzymes. This factor may be the reason that the much lower electrochemical response at higher concentration of probe (2.0 μM). Thus, 0.8 μM was chosen as the optimized immobilization concentration for the following detection.

As both the amount of targets generated from EXPAR and the length of the HCR nanowires were dependent on the reaction time, we further investigated the effects of incubation time on the duel amplification process. Firstly, the electrode modified with duplex probes was incubated in the EXPAR amplification solution for a certain period of time ranging from 0 to 150 min before being subjected to the HCR process for 2 h. As demonstrated in Fig. 2B, with the incubation time increased gradually, the peak currents rose accordingly, yet the currents started to plateau longer than 90 min. The enhanced signal within 90 min validated the feasibility of the amplification process, while the plateau phenomenon may be due to the cleavage of almost all the duplex DNA probes on the electrode surface. Therefore, a reaction time of 90 min was chosen for EXPAR reaction. Subsequently, we evaluated the hybridization time for HCR with 90 min for the EXPAR process. We can see from Fig. 2B that the peak current increased as the hybridization time changed from 0 to 60 min. Then, the peak current did not change much as the time extended to 150 min. Therefore, 90 min and 60 min were chosen as the optimum reaction time for EXAR and HCR, respectively.

3.4. Detection performance of the assay

DPV was utilized to investigate the sensitivity of the proposed method. Target DNA with different concentrations were measured under the optimized reaction condition. As illustrated in Fig. 3A, the DPV peak currents increased along with the concentration of target from 0 to 5 nM. The dependent relationship between the target and the peak current confirmed the detection principle that more original target will yield more DNAzymes assembled on the electrode surface. Fig. 3B exhibits the variation of the peak current as a function of the target concentration. The electrochemical measurements were repeated three times for each concentration of target. As demonstrated in the inset of Fig. 3B, the average peak currents showed a good linear correlation with the logarithm of DNA concentration ranging from 50 fM to 100 pM. And we achieved a detection limit of 9.4 fM for DNA according to the 3σ method. The comparison of our strategy with other reported methods was illustrated in Table S2. The satisfactory sensitivity of our biosensor can be ascribed to (1) the high amplification efficiency of EXPAR coupled with HCR of DNAzymes and (2) the integration of subsequent enzymatic reaction with sensitive electrochemical detection. The results above verified that the biosensor we fabricated can ensure ultrasensitive electrochemical detection of target DNA.

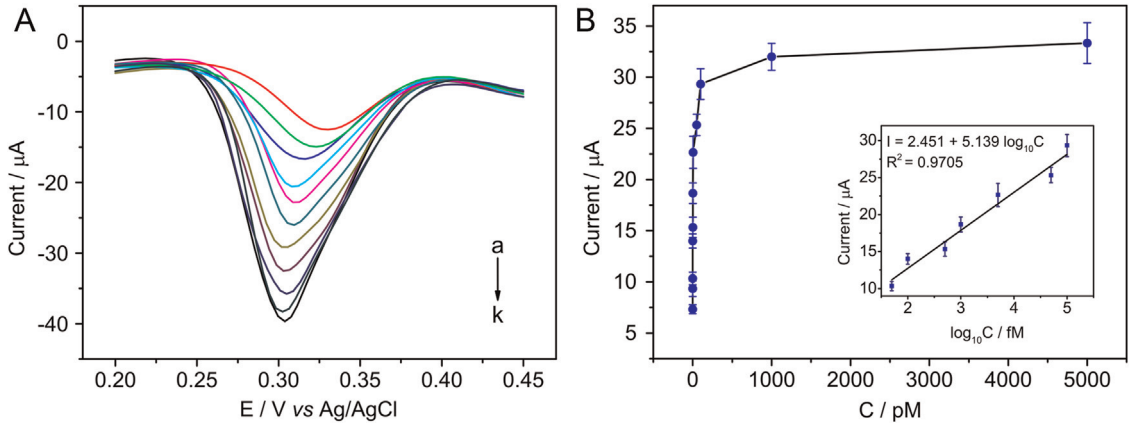

Fig. 3. (A) Differential pulse voltammograms in response to different concentrations of target DNA (a–k: 0 fM, 10 fM, 50 fM, 100 fM, 500 fM, 1 pM, 5 pM, 50 pM, 100 pM, 1 nM, and 5 nM). (B) Variation of the peak current as a function of DNA concentration. Inset: the linear relationship of currents versus the logarithm of target concentration in the range from 50 fM to 100 pM. Error bars showed the standard deviation of three experiments.

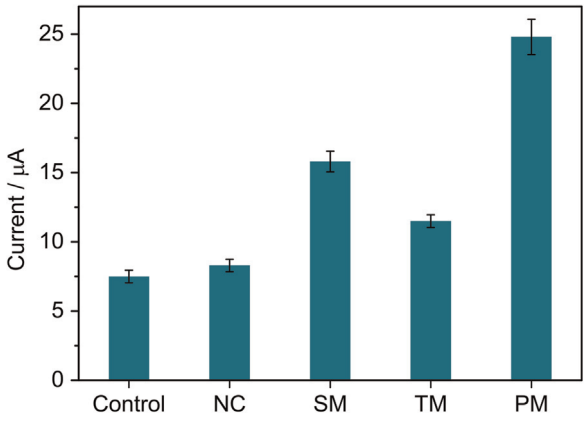

Fig. 4. Specificity investigations of blank control (Control), noncomplementary target (NC), single-base mismatched target (SM), two-base mismatched target (TM) and perfect complementary target (PM). The concentration of each sequence was 50 pM except for the blank control. Error bars were calculated from three independent experiments.

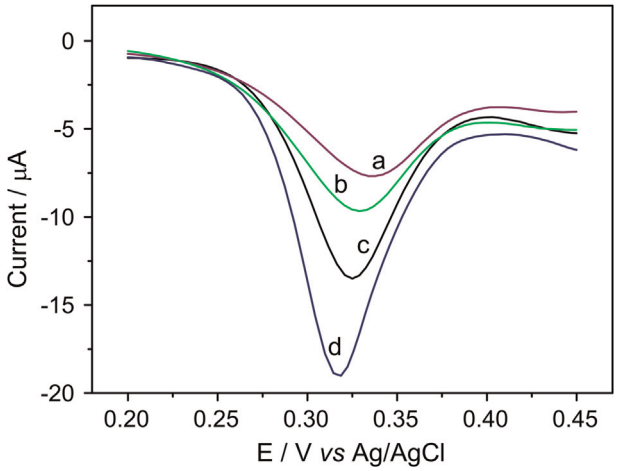

Fig. 5. Differential pulse voltammograms in response to spiked DNA in the dilution of HepG2 cell lysates at different concentrations: 0 M (a), 20 fM (b), 50 fM (c) and 500 fM (d).

SNP analysis is a great challenge of the DNA assay. To study the specificity of the proposed detection method, four kinds of DNA sequences, including target DNA, single-base mismatched target, two-base mismatched target and non-complementary sequence were selected as the detection model. The results in Fig. 4 showed that the peak currents from the non-complementary sequence was almost the same to the blank control. The signals for single-base and two-base mismatched target was only about 63.7% and 46.4% of that for target DNA, respectively. The good performance in specificity of our detection strategy gave it great potential for SNP analysis.

4. Challenged with cell lysates

We also applied our electrochemical biosensor to detect the target DNA spiked into 2:1 dilution of HepG2 cell lysates, which contained many complex components. The experiment was conducted under the optimal condition as described and the results were exhibited in Fig. 5. As shown, the peak currents increased obviously as the spiked DNA increased from 20 fM to 500 fM. In spite of the multicomponent nature of the matrix, our biosensor based on duel amplification strategy still performed excellently with well selectivity and sensitivity. Notably, the addition of 20 fM target DNA can yield a significantly enlarged response (curve b) than the base line (curve a). These results confirmed that our biosensor was competent to detect target DNA in a complex matrix.

5. Conclusions

We developed an ultrasensitive and label-free electrochemical DNA biosensor with dual-amplification strategy based on EXPAR coupled with HCR. The electrochemical platform enabled simple and ultrasensitive avian influenza A (H7N9) virus DNA sequence detection. Through the EXPAR assisted target recycling and HCR mediated self-assemble of G-quadruplex, a duel amplification process can be triggered by the target, which can yield electrochemical response after the enzymic catalytic oxidation of TMB. The proposed protocol was rather simple and time saving. It showed a broad dynamic range and can achieve ultrasensitive electrochemical detection of DNA down to 9.4 fM. Moreover, the biosensor demonstrated good selectivity in SNP discrimination as well as satisfactory performance in spiked cell lysates analysis. In view of above advantages, our strategy offered an potential option in virus diagnosis and clinical analysis.

Acknowledgments

This work was supported by the National Natural Science Foundation of China (Grant nos. 21375152 and 21075139).

Appendix A. Supplementary material

Supplementary data associated with this article can be found in the online version at http://dx.doi.org/10.1016/j.bios.2014.09.080.

References

Ahirwal, G.K., Mitra, C.K., 2010. Biosens. Bioelectron. 25 (9), 2016–2020.
Cheglakov, Z., Weizmann, Y., Basnar, B., Willner, I., 2007. Org. Biomol. Chem. 5 (2), 223–225.
Dervan, P.B., 2001. Biorg. Med. Chem. 9 (9), 2215–2235.
Duan, R., Zuo, X., Wang, S., Quan, X., Chen, D., Chen, Z., Jiang, L., Fan, C., Xia, F., 2013. J. Am. Chem. Soc. 135 (12), 4604–4607.
Gao, Y., Li, B.X., 2013. Anal. Chem. 85 (23), 11494–11500.
Ge, Z., Lin, M., Wang, P., Pei, H., Yan, J., Shi, J., Huang, Q., He, D., Fan, C., Zuo, X., 2014. Anal. Chem. 86 (4), 2124–2130.
Hun, X., Liu, F., Mei, Z., Ma, L., Wang, Z., Luo, X., 2013. Biosens. Bioelectron. 39 (1), 145–151.
Keren, K., Krueger, M., Gilad, R., Ben-Yoseph, G., Sivan, U., Braun, E., 2002. Science 297 (5578), 72–75.
Li, D., Shlyahovsky, B., Elbaz, J., Willner, I., 2007. J. Am. Chem. Soc. 129 (18), 5804–5805.
Li, T., Li, B.L., Wang, E.K., Dong, S.J., 2009. Chem. Commun. 24, 3551–3553.
Liu, M.L., Zhang, Y.Y., Chen, Y.D., Xie, Q.J., Yao, S.Z., 2008. J. Electroanal. Chem. 622 (2), 184–192.
Lu, N., Pei, H., Ge, Z., Simmons, C.R., Yan, H., Fan, C., 2012. J. Am. Chem. Soc. 134 (32), 13148–13151.
Lubin, A.A., Plaxco, K.W., 2010. Acc. Chem. Res. 43 (4), 496–505.
Luo, M., Chen, X., Zhou, G.H., Xiang, X., Chen, L., Ji, X.H., He, Z.K., 2012. Chem. Commun. 48 (8), 1126–1128.
Pan, W., Zhang, T., Yang, H., Diao, W., Li, N., Tang, B., 2013. Anal. Chem. 85 (21), 10581–10588.
Sassolas, A., Leca-Bouvier, B.D., Blum, L.J., 2008. Chem. Rev. 108 (1), 109–139.
Sharifi, E., Salimi, A., Shams, E., Noorbakhsh, A., Amini, M.K., 2014. Biosens. Bioelectron. 56, 313–319.
Shen, Q.P., Zhou, L.F., Yuan, Y.J., Huang, Y., Xiang, B.B., Chen, C.Y., Nie, Z., Yao, S.Z., 2014. Biosens. Bioelectron. 55, 187–194.
Shi, C., Liu, Q., Ma, C., Zhong, W., 2014. Anal. Chem. 86 (1), 336–339.
Shimron, S., Wang, F., Orbach, R., Willner, I., 2012. Anal. Chem. 84 (2), 1042–1048.
Wan, Y., Xu, H., Su, Y., Zhu, X., Song, S., Fan, C., 2013. Biosens. Bioelectron. 41, 526–531.

Wang, F., Lu, C.H., Liu, X., Freage, L., Willner, I., 2014a. Anal. Chem. 86 (3), 1614–1621.
Wang, G.F., He, X.P., Wang, L., Zhang, X.J., 2013. Biosens. Bioelectron. 42, 337–341.
Wang, G.L., Zhang, C.Y., 2012. Anal. Chem. 84 (16), 7037–7042.
Wang, Z.H., Lu, C.Y., Liu, J., Xu, J.J., Chen, H.Y., 2014b. Chem. Commun. 50 (10), 1178–1180.
Weizmann, Y., Beissenhirtz, M.K., Cheglakov, Z., Nowarski, R., Kotler, M., Willner, I., 2006. Angew. Chem. Int. Ed. 45 (44), 7384–7388.
Willner, I., Shlyahovsky, B., Zayats, M., Willner, B., 2008. Chem. Soc. Rev. 37 (6), 1153–1165.
Wu, M.S., He, L.J., Xu, J.J., Chen, H.Y., 2014. Anal. Chem. 86 (9), 4559–4565.
Xia, F., White, R.J., Zuo, X., Patterson, A., Xiao, Y., Kang, D., Gong, X., Plaxco, K.W., Heeger, A.J., 2010. J. Am. Chem. Soc. 132 (41), 14346–14348.
Xiao, Y., Rowe, A.A., Plaxco, K.W., 2007. J. Am. Chem. Soc. 129 (2), 262–263.
Xu, J., Jiang, B.Y., Su, J., Xiang, Y., Yuan, R., Chai, Y.Q., 2012. Chem. Commun. 48 (27), 3309–3311.
Xuan, F., Luo, X., Hsing, I.M., 2013. Anal. Chem. 85 (9), 4586–4593.
Zhang, Y., Hu, J., Zhang, C.Y., 2012. Anal. Chem. 84 (21), 9544–9549.
Zhou, M.Y., Liu, Y., Tu, Y.F., Tao, G.H., Yan, J.L., 2012. Biosens. Bioelectron. 35 (1), 489–492.
Zhou, W., Gong, X., Xiang, Y., Yuan, R., Chai, Y., 2014a. Biosens. Bioelectron. 55, 220–224.
Zhou, W.J., Su, J., Chai, Y.Q., Yuan, R., Xiang, Y., 2014b. Biosens. Bioelectron. 53, 494–498.
Zhu, W.Y., Su, X.P., Gao, X.Y., Dai, Z., Zou, X.Y., 2014. Biosens. Bioelectron. 53, 414–419.
Zhu, X., Zhao, J., Wu, Y., Shen, Z., Li, G., 2011. Anal. Chem. 83 (11), 4085–4089.